



Effect of silver thickness on structural, optical and morphological properties of nanocrystalline Ag/NiO thin films

S. Jalili¹ · F. Hajakbari¹ · A. Hojabri¹

Received: 28 August 2017 / Accepted: 25 February 2018 / Published online: 9 March 2018
© The Author(s) 2018. This article is an open access publication

Abstract

Silver (Ag) nanolayers were deposited on nickel oxide (NiO) thin films by DC magnetron sputtering. The thickness of Ag layers was in range of 20–80 nm by variation of deposition time between 10 and 40 s. X-ray diffraction results showed that the crystalline properties of the Ag/NiO films improved by increasing the Ag film thickness. Also, atomic force microscopy and field emission scanning electron microscopy images demonstrated that the surface morphology of the films was highly affected by film thickness. The film thickness and the size of particles change by elevating the Ag deposition times. The composition of films was determined by Rutherford back scattering spectroscopy. The transmission of light was gradually reduced by augmentation of Ag films thickness. Furthermore; the optical band gap of the films was also calculated from the transmittance spectra.

Keywords Sputtering · Silver · Nickel oxide · Thin films · RBS

Introduction

Nanostructured materials owing to unique physical and chemical characteristics compared with those of the bulk materials have received considerable attentions in recent years [1–3]. On the other hand, transition metal oxides semiconducting materials such as MoO₃, WO₃ and NiO have great potential application in microelectronics and optoelectronics [4–15]. Among them, nickel oxide (NiO) has specific properties and diverse applications. The properties of NiO thin films which make it suitable for the different applications are excellent durability, low material cost, wide optical band gap, excellent electrical and optical properties [7–13]. NiO thin films can be applied in electrochromic display devices, gas sensors, positive electrode in Li-ion batteries [5–10]. Several techniques have been used to prepare NiO thin films, including pulsed laser deposition [5], plasma oxidation [7], DC and RF magnetron sputtering [8–12], sol–gel [13, 14] and so on. In addition to these preparation methods, NiO films can also be prepared

by thermal oxidation of nickel film [16]. This method, compared to other techniques, is low cost, efficient and convenient. In this work, NiO thin films were fabricated on BK7 and silicon by thermal oxidation of sputtered nickel films. It is well known that the size, structure and morphology of the films are the essential parameters for those applications [17–22]. The physical properties of the metal oxide thin films could be modified by adding suitable doping materials like Li, Cu, Au and Ag [1, 14, 23]. Sta et al. [14] investigated the hydrogen sensors prepared using nickel oxide (NiO) and lithium-doped nickel oxide (NiO:Li) thin films. They found that for all hydrogen concentrations and operating temperatures, the response of the NiO:Li films is better than the response of NiO. The nanocomposite NiO:Ag thin films were deposited using pulsed laser deposition technique by Fasaki et al. [5] for gas-sensing applications. They observed that the addition of the gold nanoparticles in NiO increased the sensor sensitivity significantly. The addition of silver nanoparticles in the oxide matrix is performed in transparent conductive oxide films, gas-sensing films, photocatalytic films, and antibacterial coatings [24–26]. On the other hands metal/metal oxide multilayer play an important role in the micro- and nanoelectronics and optoelectronics [24–27]. Metallic or low band gap nanoparticles serve as the

✉ F. Hajakbari
fatemeh.hajakbari@kiaou.ac.ir

¹ Department of Physics, Karaj Branch, Islamic Azad University, Karaj, Iran

nanoelectrodes [28]. Deposition of metallic nanoelectrodes on the solid state gas sensors can influence the sensitivity of them [28, 29]. Therefore, in this study, Ag nanolayers were deposited on NiO thin films and the objective of the present study is investigating the effects of Ag layer thickness on the crystalline structure, surface morphology, and optical properties of Ag/NiO thin films.

Experimental methods

The NiO thin films were prepared by the following procedure. In the first step, nickel (Ni) thin films were deposited by DC magnetron sputtering onto BK7 and silicon substrates using a Ni target (77 mm diameter and 3 mm thickness) (99.999% purity). Then, the Ni films were annealed in an electrical furnace for 4 h at 500 °C to prepare the NiO films. The deposition conditions of Ni films are as follows. The distance between the target and the substrate was 4.2 cm. Before the sputtering, the chamber was evacuated to a base pressure of 7.3×10^{-5} mbar using diffusion and rotary pumps. Pure argon was used as the working gas. The working pressure was 7×10^{-2} mbar and the sputtering voltage and discharge current were 200 V and 20 mA, respectively. The substrates were cleaned ultrasonically in ethanol and acetone for 10 min before introducing them into the deposition chamber. The deposition time was 70 min for all the prepared samples. Finally, the Ag films were deposited on NiO films by DC magnetron sputtering in accordance with the conditions shown in Table 1. The thickness of Ag layers was in range of 20–80 nm by fixing the deposition rate at 2 nm/s and variation of deposition time between 10 and 40 s. The films deposited on BK7 substrates were introduced as samples, B0 ($t = 0$ s), B1 ($t = 10$ s), B2 ($t = 30$ s) and B3 ($t = 40$ s). Phase identification and structural properties of the films were studied by X-ray diffraction (XRD; Philips PW 3710) analysis with Co radiation ($\lambda = 0.17890$ nm). For the surface morphological studies of the films, atomic force microscopy (AFM; Park Scientific Instruments Auto Probe

CP) in contact mode and field emission scanning electron microscopy (FESEM; HitachiS-4160) were employed. Also, to study the surface features of prepared films, the main surface roughness parameters of these films, including root mean square (RMS) and average roughness (R_a) were measured by AFM analysis. The composition of different layers were determined by Rutherford back scattering spectroscopy (RBS) using a 2 MeV proton beam of a 3 MV single-ended Van de Graff machine. The scattered particles were measured using a surface barrier detector at 165°. Numerical analysis of the collected data was performed via the SIMNRA simulation package [24]. The optical transmittance of the NiO and Ag/NiO thin films on BK7 substrates was measured using a spectrophotometer (UV ikon 922) in the wavelength range of 200–1100 nm.

Results and discussion

Structural properties

In order to determine the structure and crystallinity of the prepared films, XRD analysis was employed. The XRD patterns of pure NiO and Ag/NiO thin films deposited on BK7 substrates are shown in Fig. 1. The XRD data indicates that all the pure NiO and Ag/NiO thin films having polycrystalline nature. A peak belonging to the NiO crystalline structure in the (200) crystallography direction (JCPDS card No. 78-0643) can be observed in XRD pattern of NiO film deposited on BK7. After deposition of Ag on NiO films at various deposition times, in addition to the NiO (200) peak, (111) reflection of silver (JCPDS card No. 87-0720) can be observed in all the films. The intensity of these peaks is found to increase for the higher values of Ag

Table 1 Deposition conditions of Ag films on nickel oxide

Target	Ag
Substrate	NiO
Base pressure (mbar)	1.2×10^{-4}
Working pressure (mbar)	5.5×10^{-2}
Voltage (V)	170
Current (A)	0.18
Deposition time (s)	10, 30, 40

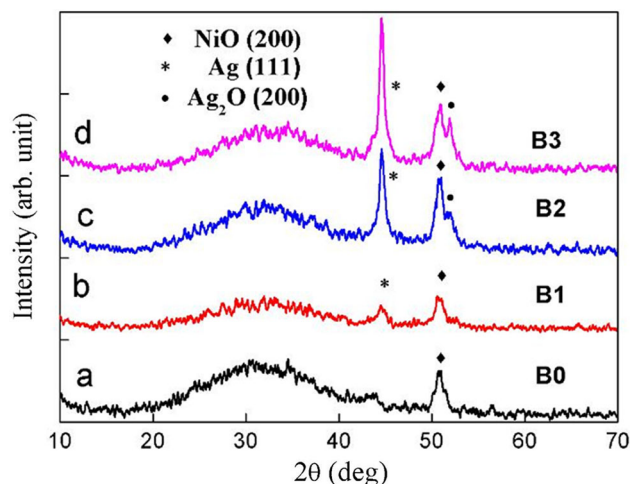
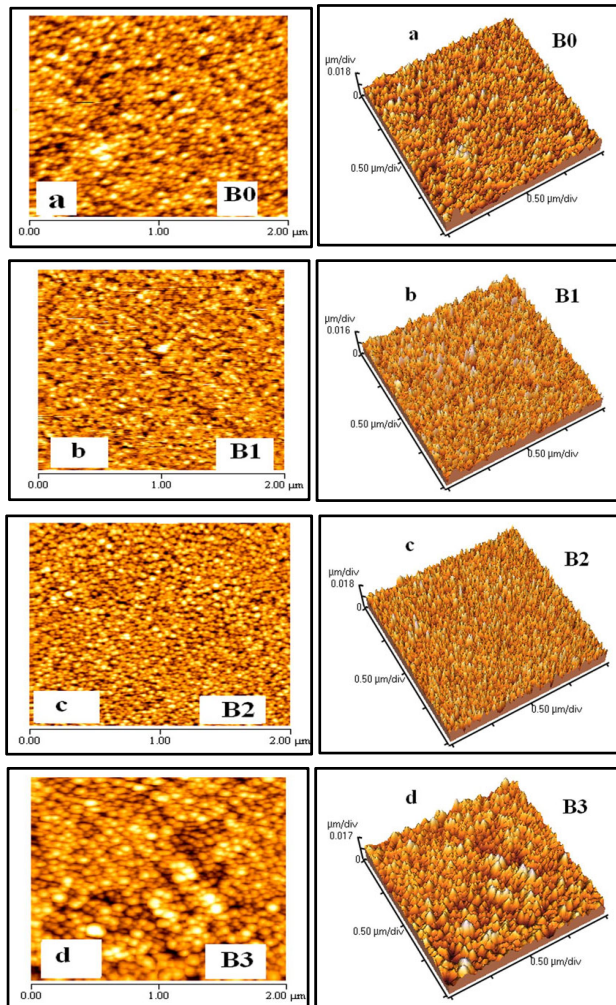


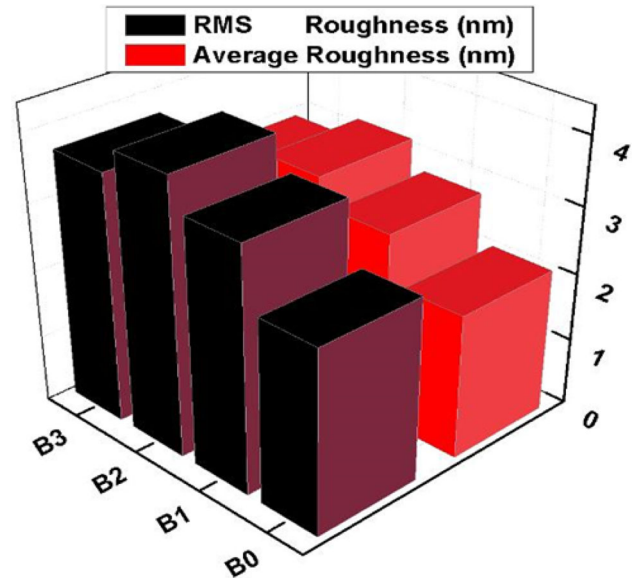
Fig. 1 XRD diffraction patterns of **a** NiO film, and Ag/NiO films on BK7 for different Ag film thicknesses **b** 20 nm, **c** 60 nm and **d** 80 nm

Table 2 Summary of structural data obtained for Ag/NiO thin films

Sample number	Diffraction angle 2θ (deg)	Phase composition	Miller indices (hkl)	FWHM (rad)	Average crystallite size (nm)	Microstrain ϵ ($\times 10^{-3}$)	Dislocation density δ ($\times 10^{+15}$ lines/m ²)
B0	50.86	NiO	(200)	0.0137	13.01	7.20	5.9
B1	44.50	Ag	(111)	0.0158	11.00	9.65	8.2
B1	50.51	NiO	(200)	0.0146	12.20	7.74	6.7
B2	44.60	Ag	(111)	0.0108	16.10	6.58	3.8
B3	44.60	Ag	(111)	0.0106	16.40	6.46	3.7

**Fig. 2** 2D and 3D AFM images of **a** NiO film, and Ag/NiO films on BK7 for different Ag film thicknesses **b** B1: 20 nm, **c** B2: 60 nm and **d** B3: 80 nm

thickness and it attributed to improvement of films crystallinity. On the other hand, a new peak corresponding to Ag₂O (200) is appeared in XRD patterns after the deposition time of 30 s. To obtain more information regarding the structural quality of prepared Ag/NiO thin film, some

**Fig. 3** The plot of RMS and average roughnesses of (B0) NiO film, and Ag/NiO films on BK7 for different Ag film thicknesses: B1: 20 nm, B2: 60 nm and B3: 80 nm

structural calculations have been made. The average crystallite size (D), microstrain (ϵ) and dislocation density (δ) were calculated in accordance with the following Debye–Scherrer equations [24].

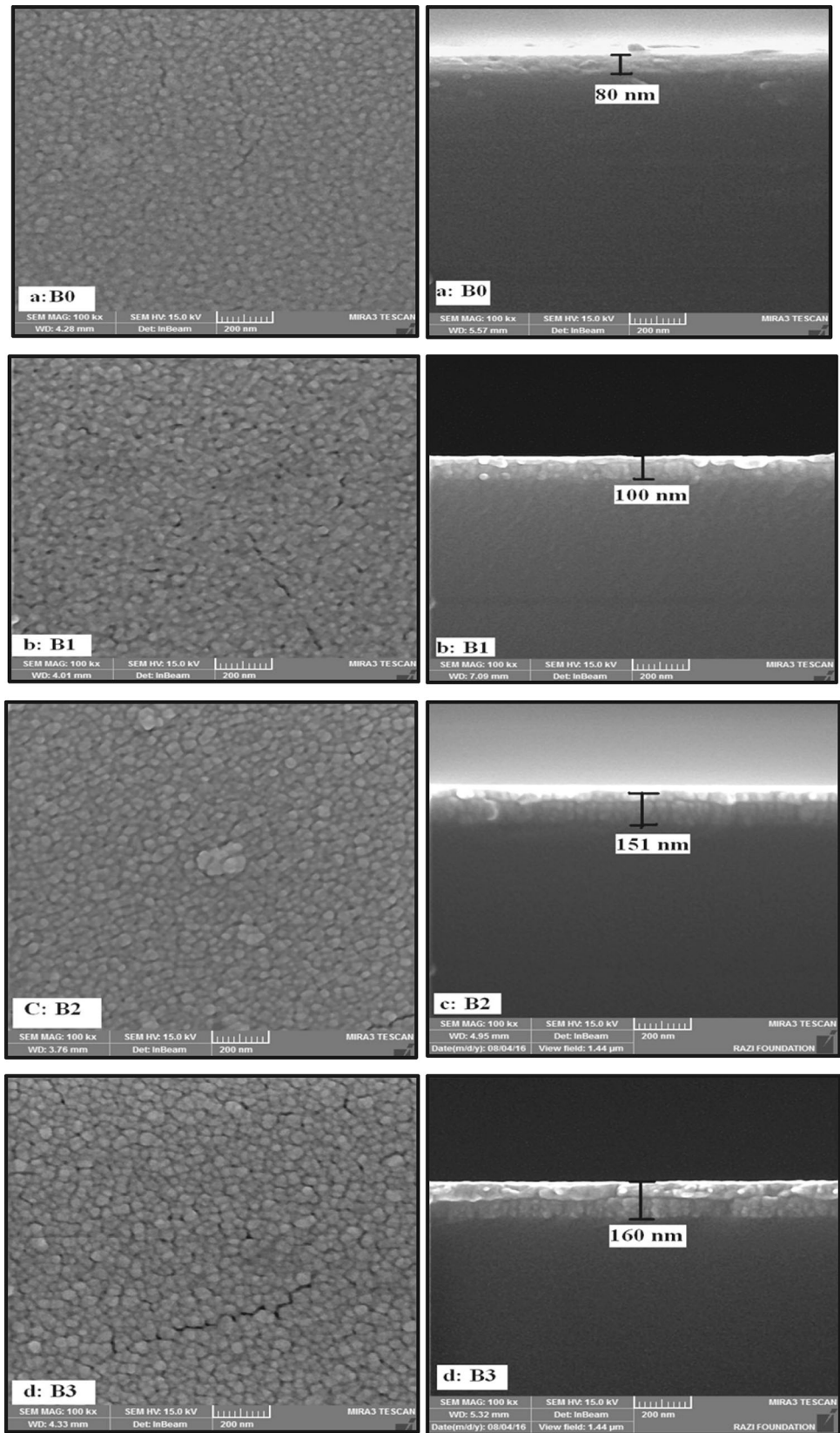
$$D = \frac{0.9\lambda}{\beta \cos \theta} \quad (1)$$

$$\epsilon = \frac{\beta}{4 \tan \theta} \quad (2)$$

$$\delta = \frac{1}{D^2}, \quad (3)$$

where β is the full width at half maximum (FWHM) of the diffraction peak, λ is the wavelength of the Co K α radiation ($\lambda = 0.17890$ nm), and θ is Bragg's angle. The calculated values of structural parameters are listed in Table 2. The crystallite size of NiO and Ag₂O particles in deposition time of 30 and 40 s could not be estimated using the Debye–Scherrer equation, because of the partial overlap of

Fig. 4 Top view (left) and cross-sectional (right) FESEM images of **a** NiO thin film, and Ag/NiO thin films deposited on BK7 for different Ag film thicknesses **b** 20 nm, **c** 60 nm and **d** 80 nm



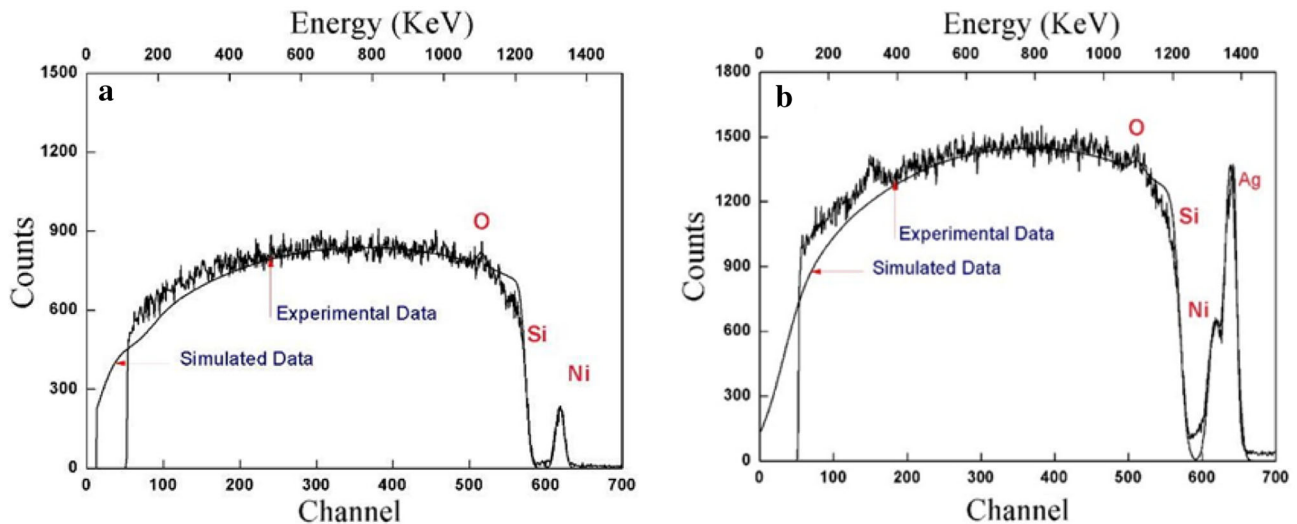


Fig. 5 RBS images of **a** NiO thin film and **b** Ag/NiO thin film deposited on silicon substrate

two peaks corresponding to NiO and Ag₂O in the diffractogram. It can be seen in Table 2 that the crystallite size is in the range of 11–16 nm, which confirms the presence of nanocrystals in the Ag/NiO films prepared in this study. Also, the dislocation density and strain are observed to decrease with deposition time. This may be due to the movement of interstitial atoms from its grain boundary to the crystallites, which may lead to reduction in the concentration of lattice defects [30].

Morphological properties

The surface morphology of pure NiO and Ag/NiO thin films was characterized by AFM analysis. The obtained three- and two-dimensional (3D and 2D) AFM images of the samples on BK7 substrates over a $2 \times 2 \mu\text{m}^2$ area are shown in Fig. 2. AFM 2D images of the Ag/NiO films indicate different morphologies of surface grains, which depend on the Ag films thickness and the grain size increases with augmentation of deposition time which can be related to the agglomeration of crystallites. According to AFM 3D images, we can observe that the growth of layers was pyramidal for all samples. Figure 3 exhibits the plot of RMS and average roughness of the prepared films. According to surface roughness values shown in this figure, we can observe that the RMS and average roughness follow the similar trends.

FESEM analysis

To further explore the surface microstructure evolution of the prepared films, the top view and cross-sectional FESEM images of the NiO and Ag/NiO films grown on BK7 are presented in Fig. 4. The images show that the

surface of films is uniform, and homogeneous and films consist of dense layers. Cross-sectional FESEM images exhibit the films thickness increases with increasing the deposition time of Ag and augmentation in the films thickness promote the agglomeration of particles and the size of particles increases. The results obtained in FESEM are in agreement with the results of AFM and XRD.

RBS analysis

For determination of films composition, RBS was performed. The experimental RBS spectra of NiO (sample B0) and Ag/NiO (sample B2) thin films on silicon substrates along with simulated curves calculated by SIMNRA cod are shown in Fig. 5a, b. RBS has been done on films deposited on silicon due to the ease of simulation on silicon wafers. The signals of the elements of the film such as Ni, O as well as Si substrate are clearly observed in the RBS spectrum of NiO thin film (Fig. 5a). After deposition of Ag on NiO, the signals of the constituents of the films such as Ag, Ni, O, and the silicon substrate are observed in the RBS spectra (Fig. 5b). Furthermore, the ion scattering from Ag atoms occurs at higher backscattering energy. This is because the backscattered energy of the incident ions is depending on the atomic mass of the elements from which the ions backscatters [31]. The atomic masses of the elements are 15.99, 28.09, 58.69 and 107.87 for O, Si, Ni and Ag, respectively, and the Ag is the heaviest among the elements either in the films or in the substrate. On the other hand, the broadness and intensity of the RBS peaks are related to films thickness and concentration of backscattered ions, respectively [31]. The RBS spectra clearly show that the Ag/NiO film thickness is larger than the NiO films. These results are consistency with the FESEM results.

Optical studies

To investigate the influence of Ag film thickness on the optical properties of Ag/NiO films, the transmittance spectra of the NiO and Ag/NiO thin films were recorded at room temperature, in the wavelength range of 200–1100 nm. The normal-incidence transmittance spectra of the films deposited on BK7 are shown in Fig. 6. It is apparent from the figure that the maximum transmittance is belonging to NiO film and the transmittance of the Ag/NiO films in the visible region decreases with increasing the Ag film thickness. According to cross-sectional FESEM results the Ag/NiO films thickness increased with augmentation in deposition times and the thicker film is denser and being

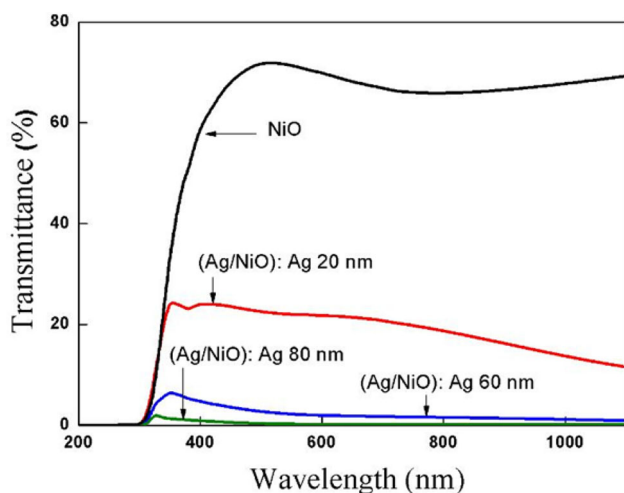
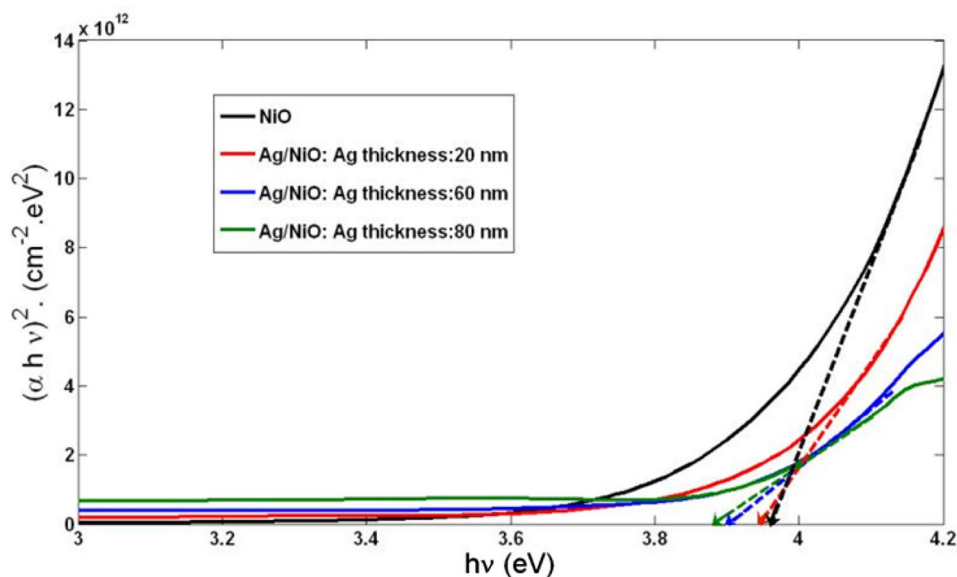


Fig. 6 Transmission spectra of NiO and Ag/NiO thin films deposited on BK7 substrates

Fig. 7 $(\alpha h\nu)^2$ versus $(h\nu)$ plot of NiO and Ag/NiO thin films deposited on BK7 substrates



more defective results in a decrease in film transparency. The transmittance peaks of Ag/NiO films are around 352, 354 and 329 nm, respectively. In the short wavelength region, the transmittance is affected by light absorption caused by inter-band electronic transitions. When the deposition time of Ag increases, the Ag layer thickness enhances in the Ag/NiO films and, therefore, more electrons are available for inter-band transitions and more light absorption can occur. In the long wavelength region, the transmittance is affected by Ag layer reflection resulting in the reduced transmittance.

Now, we attempt to gain optical band gap information. In the fundamental absorption region, the optical absorption coefficient (α) was calculated from the optical transmittance (T) data using $\alpha = (1/d) \ln(1/T)$, where d is the film thickness and T is the transmittance. The optical band gap (E_g) of the films was determined from the plot of $(\alpha h\nu)^2$ versus photon energy ($h\nu$) using Tauc's relation [32]. An extrapolation of the linear region of this plot to $\alpha = 0$ gives the value of the band gap. Figure 7 shows the plot of $(\alpha h\nu)^2$ versus photon energy of NiO and Ag/NiO thin films prepared at different deposition time of Ag. The direct optical band gaps were found to be 3.97, 3.95, 3.90 and 3.88 eV for samples B0, B1, B2 and B3, respectively. The band gap values obtained in this investigation closely match with the values reported in the literature [11, 13, 15]. In addition, the band gap value decreases with increasing film thickness due to increase in grain size. A similar variation in optical band gap with film thickness was reported by Matheswaran et al. [33]. The above results show that the film thickness and morphology have direct influences on optical transmittance and optical band gap of Ag/NiO films.

Conclusions

In this investigation, nanolayers of Ag were deposited on NiO by DC magnetron sputtering. The effects of Ag layer deposition time on Ag/NiO film thickness, structure, surface morphology, and optical properties were studied. The XRD patterns showed that an increase in the Ag film thickness led to formation of the nanocrystalline mixed phase of Ag, NiO, and Ag₂O and improvement of the films crystallinity. The FESEM and AFM images exhibited a significant change in surface morphology by elevation in Ag film thickness. The RBS elemental studies confirmed the existence of Ag, Ni and O in Ag/NiO films. The optical band gap values of the films decreased from 3.97 to 3.88 eV with increasing the film thickness.

Acknowledgements This work was supported by the Islamic Azad University, Karaj Branch, Karaj, Iran.

Open Access This article is distributed under the terms of the Creative Commons Attribution 4.0 International License (<http://creativecommons.org/licenses/by/4.0/>), which permits unrestricted use, distribution, and reproduction in any medium, provided you give appropriate credit to the original author(s) and the source, provide a link to the Creative Commons license, and indicate if changes were made.

References

- Kumar, G.S., Illyaskutty, N., Suresh, S., Sreedharan, R.S., Nayar, V.U., Pillai, V.M.: Terbium oxide doped MoO₃ nanostructures: Morphology engineering and enhanced photoluminescence. *J. Alloys Compd.* **698**, 215–227 (2017)
- Mishra, P.P., Raja, M.M., Panda, R.N.: Novel synthesis, characterization and magnetic properties of nano-structured γ -Mo₂N and γ -Co_{0.25}Mo_{1.75}N nitrides. *Mater. Res. Bull.* **86**, 241–247 (2017)
- Jasbi, N.E., Dorrnian, D.: Effect of aging on the properties of TiO₂ nanoparticle. *J. Theor. Appl. Phys.* **10**, 157–161 (2016)
- Sun, J., Zheng, Q., Cheng, S., Zhou, H., Lai, Y., Yu, J.: Comparing molybdenum oxide thin films prepared by magnetron sputtering and thermal evaporation applied in organic solar cells. *J. Mater. Sci. Mater. Electron.* **27**, 3245–3249 (2016)
- Fasaki, I., Kandyla, M., Kompitsas, M.: Properties of pulsed laser deposited nanocomposite NiO: Au thin films for gas sensing applications. *Appl. Phys. A* **107**, 899–904 (2012)
- Cao, L., Wang, D., Wang, R.: NiO thin films grown directly on Cu foils by pulsed laser deposition as anode materials for lithium ion batteries. *Mater. Lett.* **132**, 357–360 (2014)
- Rashvand, S., Hojabri, A.: Structural, morphological and optical properties of nanostructure nickel oxide thin films on quartz substrates grown by plasma oxidation. *J. Inorg. Organomet. Polym.* **27**(2), 503–509 (2017)
- Karpinski, A., Ferrec, A., Plouet, M.R., Cattin, L., Djouadi, M.A., Brohan, L., Jouan, P.Y.: Deposition of nickel oxide by direct current reactive sputtering: Effect of oxygen partial pressure. *Thin Solid Films* **520**, 3609–3613 (2012)
- Peng, T.C., Xiao, X.H., Han, X.Y., Zhou, X.D., Wu, W., Ren, F., Jiang, C.Z.: Characterization of DC reactive magnetron sputtered NiO films using spectroscopic ellipsometry. *Appl. Surf. Sci.* **257**, 5908–5912 (2011)
- Reddy, A.M., Reddy, A.S., Lee, K.S., Reddy, P.S.: Effect of oxygen partial pressure on the structural, optical and electrical properties of sputtered NiO films. *Ceram. Int.* **37**, 2837–2843 (2011)
- Ai, L., Fang, G., Yuan, L., Liu, N., Wang, M., Li, C., Zhang, Q., Li, J., Zhao, X.: Influence of substrate temperature on electrical and optical properties of p-type semitransparent conductive nickel oxide thin films deposited by radio frequency sputtering. *Appl. Surf. Sci.* **254**, 2401–2405 (2008)
- Ahmed, A.A., Devarajan, M., Afzal, N.: Effects of substrate temperature on the degradation of RF sputtered NiO properties. *Mater. Sci. Semicond. Process.* **63**, 137–141 (2017)
- Raut, B.T., Pawar, S.G., Chougule, M.A., Sen, S., Patil, V.B.: New process for synthesis of nickel oxide thin films and their characterization. *J. Alloys Compd.* **509**, 9065–9070 (2011)
- Sta, I., Jlassi, M., Kandyla, M., Hajji, M., Koralli, P., Allagui, R., Kompitsas, M., Ezzaouia, H.: Hydrogen sensing by sol-gel grown NiO and NiO: Li thin films. *J. Alloys Compd.* **626**, 87–92 (2015)
- Anandan, K., Rajendran, V.: Morphological and size effects of NiO nanoparticles via solvothermal process and their optical properties. *Mater. Sci. Semicond. Process.* **14**, 43–47 (2011)
- Hajakbari, F., Afzali, M.T., Hojabri, A.: Nanocrystalline nickel oxide (NiO) thin films grown on quartz substrates: Influence of annealing temperatures. *Acta Phys. Pol. A* **131**(3), 417–419 (2017)
- Sadeghi, H., Dorrnian, D.: Influence of size and morphology on the optical properties of carbon nanostructures. *J. Theor. Appl. Phys.* **10**, 7–13 (2016)
- Wang, J., Yang, P., Wei, X., Zhou, Z.: Preparation of NiO two-dimensional grainy films and their high-performance gas sensors for ammonia detection. *Nanoscale Res. Lett.* **10**, 119–223 (2015)
- Solati, E., Dorrnian, D.: Comparison between silver and gold nanoparticles prepared by pulsed laser ablation in distilled water. *J. Cluster Sci.* **26**(3), 727–742 (2015)
- Mani Menaka, S., Umadevi, G., Manickam, M.: Effect of copper concentration on the physical properties of copper doped NiO thin films deposited by spray pyrolysis. *Mater. Chem. Phys.* **191**, 181–187 (2017)
- Sari, A.H., Ghorbani, S., Dorrnian, D., Azadfar, P., Hojabri, A.: Formation of SiC using low energy CO₂ ion implantation in silicon. *Appl. Surf. Sci.* **255**(5), 2180–2184 (2008)
- Hojabri, A., Haghghian, N., Yasserian, K., Ghoranneviss, M.: The effect of nitrogen plasma on copper thin film deposited by DC magnetron sputtering. *IOP Conf. Ser. Mater. Sci. Eng.* **12**, 012004–012007 (2010)
- Hojabri, A., Adavi, M., Hajakbari, F.: Synthesis of nickel-doped TiO₂ thin films and their structural and optical properties at different annealing temperatures. *Acta Phys. Pol. A* **131**(3), 386–388 (2017)
- Hajakbari, F., Shafienejad, F.: Structural, morphological, electrical, and optical properties of silver thin films of varying thickness deposited on cupric oxide. *Jpn. J. Appl. Phys.* **55**(3), 035503 (2016)
- Al-Kuhaili, M.F., Ahmad, S.H.A., Durrani, S.M.A., Faiz, M.M., Ul-Hamid, A.: Application of nickel oxide thin films in NiO/Ag multilayer energy-efficient coatings. *Mater. Sci. Semicond. Process.* **39**, 84–89 (2015)
- Sivaramakrishna, K., Ngo, A.T., Lyer, S., Alford, T.L.: Effect of thermal processing on silver thin films of varying thickness deposited on zinc oxide and indium tin oxide. *J. Appl. Phys.* **105**, 063525 (2009)



27. Chua, C.H., Wu, H.W., Huang, J.L.: Study of Cu-based Al-doped ZnO multilayer thin films with different annealing conditions. *Ceram. Int.* **42**, 5754–5761 (2016)
28. Tricoli, A., Pratsinis, S.E.: Dispersed nanoelectrode devices. *Nat. Nanotechnol.* **5**, 54–60 (2010)
29. Chen, H.I., Hsiao, C.Y., Chen, W.C., Chang, C.H., Chou, T.C., Liu, I.P., Lin, K.W., Liu, W.C.: Characteristics of a Pt/NiO thin film-based ammonia gas sensor. *Sens. Actuator B Chem.* **256**, 962–967 (2018)
30. Teh, Y.C., Saif, A.A.: Influence of annealing temperature on structural and optical properties of sol-gel derived $\text{Ba}_{0.9}\text{Gd}_{0.1}\text{-TiO}_3$ thin films for optoelectronics. *J. Alloys Compd.* **703**, 407–413 (2017)
31. Hojabri, A.: Structural and optical characterization of ZrO_2 thin films grown on silicon and quartz substrates. *J. Theor. Appl. Phys.* **10**, 219–224 (2016)
32. Tauc, J., Menth, A.: States in the gap. *J. Non-Cryst. Solids* **8**, 569 (1972)
33. Matheswaran, P., Gokul, B., Abhirami, K.M., Sathyamoorthy, R.: Thickness dependent structural and optical properties of In/Te bilayer thin films. *Mater. Sci. Semicond. Process.* **15**, 486–491 (2012)

Publisher's Note

Springer Nature remains neutral with regard to jurisdictional claims in published maps and institutional affiliations.